Understanding the electric and magnetic response of isolated metaatoms by means of a multipolar field decomposition

J. Petschulat, Jianji Yang, C. Menzel, C. Rockstuhl, A. Chipouline, Philippe Lalanne, A. Tünnermann, F. Lederer, T. Pertsch

Understanding the electric and magnetic response of isolated metaatoms by means of a multipolar field decomposition

J. Petschulat[1*], J. Yang[2], C. Menzel[3], C. Rockstuhl[3], A. Chipouline[1], P. Lalanne[2], A. Tünnermann[1], F. Lederer[3], and T. Pertsch[1]

[1] *Institute of Applied Physics, Friedrich-Schiller-Universität Jena, Max Wien Platz 1, 07743, Jena, Germany*

[2] *Laboratoire Charles Fabry de l'Institut d'Optique, Universitè Paris-Sud, 91127 Palaiseau Cedex, France*

[3] *Institute of Condensed Matter Theory and Solid State Optics, Friedrich-Schiller-Universität Jena, Max Wien Platz 1, 07743, Jena, Germany*

[*] *joerg.petschulat@uni-jena.de*

Abstract: We introduce a technique to decompose the scattered near field of two-dimensional arbitrary metaatoms into its multipole contributions. To this end we expand the scattered field upon plane wave illumination into cylindrical harmonics as known from Mie's theory. By relating these cylindrical harmonics to the field radiated by Cartesian multipoles, the contribution of the lowest order electric and magnetic multipoles can be identified. Revealing these multipoles is essential for the design of metamaterials because they largely determine the character of light propagation. In particular, having this information at hand it is straightforward to distinguish between effects that result either from the arrangement of the metaatoms or from their particular design.

OCIS codes: (160.3918) Metamaterials; (290.4020) Mie theory.

References

1. S. Linden, C. Enkrich, M. Wegener, J. Zhou, T. Koschny, and C. M. Soukoulis, "Magnetic Response of Metamaterials at 100 Terahertz," Science **306,** 1351-1352 (2004).
2. N.-H. Shen, S. Foteinopoulou, M. Kafesaki, T. Koschny, E. Ozbay, E. N. Economou, and C. M. Soukoulis, "Compact planar far-field superlens based on anisotropic left-handed metamaterials," Phys. Rev. B **80,** 115123 (2009).
3. S. Xiao, U. K. Chettiar, A. V. Kildishev, V. P. Drachev, and V. M. Shalaev, "Yellow-light negative-index metamaterials," Opt. Lett. **34,** 3478-3480 (2009).
4. J. Valentine, S. Zhang, T. Zentgraf, E. Ulin-Avila, D. A. Genov, G. Bartal, and X. Zhang, "Three-dimensional optical metamaterial with a negative refractive index," Nature **455**, 376-380 (2008).
5. N. Liu, H. Guo, L. Fu, S. Kaiser, H. Schweizer, and H. Giessen, "Three-dimensional photonic metamaterials at optical frequencies," Nature Mat. **7,** 31-37 (2008).
6. D. J. Cho, F. Wang, X. Zhang, and Y. R. Shen, "Contribution of the electric quadrupole resonance in optical metamaterials," Phys. Rev. B **78,** 121101(R) (2008).
7. J. Petschulat, C. Menzel, A. Chipouline, C. Rockstuhl, A. Tünnermann, F. Lederer, and T. Pertsch, "Multipole approach to metamaterials," Phys. Rev. A **78,** 043811 (2008).
8. K. Vynck, D. Felbacq, E. Centeno, A. I. Cabuz, D. Cassagne, and B. Guizal, "All-Dielectric Rod-Type Metamaterials at Optical Frequencies," Phys. Rev. Lett. **102,** 133901 (2009).
9. M. Burresi, D. V. Oosten, T. Kampfrath, H. Schoenmaker, R. Heideman, A. Leinse, and L. Kuipers, "Probing the Magnetic Field of Light at Optical Frequencies," Science **326,** 550-553 (2009).

#126749 - $15.00 USD Received 9 Apr 2010; accepted 24 May 2010; published 22 Jun 2010

10. M. Decker, S. Burger, S. Linden, and M. Wegener, "Magnetization waves in split-ring-resonator arrays: Evidence for retardation effects," Phys. Rev. B **80,** 193102 (2009).
11. N. Papasimakis, V. A. Fedotov, Y. H. Fu, D. P. Tsai, and N. I. Zheludev, "Coherent and incoherent metamaterials and order-disorder transitions," Phys. Rev. B **80,** 041102(R) (2009).
12. N. Liu, H. Liu, S. Zhu, and H. Giessen, "Stereometamaterials," Nature Photon. **3,** 157-162 (2009).
13. J. Petschulat, A. Chipouline, A. Tünnermann, T. Pertsch, C. Menzel, C. Rockstuhl, and F. Lederer, "Multipole nonlinearity of metamaterials," Phys. Rev. A **80**, 063828 (2009).
14. Y. Zeng, C. Dineen, and J. V. Moloney, "Magnetic dipole moments in single and coupled split-ring resonators," Phys. Rev. B **81,** 075116 (2010).
15. A. Serdyukov, I. Semchenko, S. Tretyakov, A. Sihvola, *Electromagnetics of bi-anisotropic materials: Theory and applications* (Gordon and Breach, Amsterdam, 2001).
16. C. Helgert, C. Rockstuhl, C. Etrich, C. Menzel, E.-B. Kley, A. Tünnermann, F. Lederer, and T. Pertsch, "Effective properties of amorphous metamaterials," Phys. Rev. B **79** 233107 (2009).
17. G. Mie, "Beiträge zur Optik trüber Medien, speziell kolloidaler Metallösungen," Ann. Phys. **25,** 377-445 (1908).
18. J. D. Jackson, *Classical Electrodynamics* (Wiley, New York, 1975).
19. R. E. Raab and O. L. D. Lange, *Multipole Theory in Electromagnetism* (Clarendon, Oxford, 2005).
20. N. Liu, L. Langguth, T. Weiss, J. Kästel, M. Fleischhauer, T. Pfau and H. Giessen, "Plasmonic analogue of electromagnetically induced transparency at the Drude damping limit," Nature Mat. **8,** 758-762 (2009).
21. P. B. Johnson and R. W. Christy, "Optical Constants of Noble Metals," Phys. Rev. B **6,** 4370-4379 (1972).
22. We applied the commercial product COMSOL. (www.comsol.com)
23. M. Husnik, M. W. Klein, N. Feth, M. König, J. Niegemann, K. Busch, S. Linden, and M. Wegener, "Absolute extinction cross-section of individual magnetic split-ring resonators," Nature Photon. **2,** 614-617 (2008).
24. M. Celebrano, M. Savoini, P. Biagioni, M. Zavelani-Rossi, P.-M. Adam, L. Duo, G. Cerullo, and M. Finazzi, "Retrieving the complex polarizability of single plasmonic nanoresonators," Phys. Rev. B **80,** 153407 (2009).
25. C. F. Bohren and D. R. Huffman, *Absorption and Scattering of Light by Small Particles* (Wiley, New York, 1983).
26. O. J. F. Martin and N. B. Piller, "Electromagnetic scattering in polarizable backgrounds," Phys. Rev. E **58,** 3909-3915 (1998).
27. I. S. Gradstein and I. M. Ryshik, *Tables of Series, Products and Integrals* (Harry Deutsch, Frankfurt, 1981).

1. Introduction

Metamaterials may be understood as a kind of artificial matter that allows to control the mould of light predominantly by the geometry of their building blocks rather by their intrinsic material properties. Fascination arose since these building blocks, commonly called the metaatoms, can be designed to allow for propagation effects inaccessible in natural materials. To simply describe the optical action of metamaterials, effective properties are in most cases assigned that are retrieved from the optical response of an ensemble of metaatoms instead from these individual atoms themselves. For this purpose, single layer [1–3] or bulk metamaterials [4, 5] are usually treated as black boxes to which effective properties are assigned with the only purpose to reproduce scattering data like reflection and transmission coefficients. These data do not provide sufficient insights into the physics of metamaterials since their rational design usually aims at evoking a certain multipolar scattering response [6–8]. Although metamaterials cover a wide range of structures at present, media with a magnetic response [9, 10] at optical frequencies are particularly appealing since they do not exist in nature. The pertinent metaatoms shall then possess a strong magnetic dipole moment. To achieve this, the metaatoms are typically ring-shaped [11], resulting in a ring-like current distribution at resonance. Hence, the optical response contains a strong magnetic dipole field contribution leading to an appreciable dispersion in the effective permeability. Such understanding of metamaterials is very versatile as it provides the possibility to optimize metaatoms for different spectral domains [12].

The advantage of understanding the optical response in terms of multipole scattering is furthermore proven by various theoretical works [6–8, 13–15]. It was shown that the optical response of single metamaterial layers as well as of bulk metamaterials can be described by assuming induced multipole moment densities up to the second order. From the multipolar contributions of the field scattered by the metaatoms it is even possible to directly assign effective material parameters. Even the effects of disorder can be studied and understood in terms

#126749 - $15.00 USD Received 9 Apr 2010; accepted 24 May 2010; published 22 Jun 2010

of a multipole analysis as shown theoretically and experimentally [16]. Hence, a detailed quantitative theoretical study of the optical response of the single metaatom is appropriate and in most cases sufficient to deduce the optical response of an ensemble of these entities. Although important, such a contribution is currently missing. Whereas first attempts are reported in literature [14] the analysis was usually restricted to the far-field scattering response. Then, either by optimizing the magnitude of the different multipolar contributions to match a certain angular scattering response or by probing for the scattering strength in certain directions where some multipole moments do not radiate, the multipolar response can be revealed. Nevertheless, it remains an open question how unique the assignments based on the far fields are.

In this contribution we develop a rigorous method to analyze the scattered near-field of individual metaatoms that permits disclosing their multipolar scattering contributions. The key ingredient is an expansion of the scattered field of the metaatoms upon plane wave illumination into cylindrical harmonics, i.e., we are restricting the current analysis to two-dimensional metaatoms. By relating these cylindrical harmonics to the field of Cartesian multipoles, it is possible to calculate their spectrally resolved amplitudes. With this method at hand we will subsequently investigate the multipole contributions to the scattered field of two prominent and frequently studied metaatoms providing artificial magnetism; namely the split-ring resonator (SRR) and the cut-wire pair (CW). It is shown that the scattering response contains contributions of electric and magnetic dipoles, but also of an electric quadrupole. It resonates simultaneously with the magnetic dipole and its contribution is much stronger for the CW when compared to the SRR.

Although we are focussing here only on the analysis of two specific metaatoms, the present technique is general and can be applied to various other metaatoms as well. Perspectively it will permit to design metaatoms with specific predefined multipolar contributions to the scattered field and represent a tool to distinguish between properties emerging from the periodic arrangement of metaatoms or from the specific metaatom scattering response. This will be of particular importance for the prediction of effective properties of self-organized, bottom-up metamaterials which might not allow for a perfectly periodic metaatom arrangement.

2. Multipole expansion of the two-dimensional scattered field

In order to reveal the multipolar character of the field scattered by an arbitrary shaped metaatom, we will develop a method to expand its scattered field into multipole fields. Since we focus here on two-dimensional structures, cylindrical harmonics are an appropriate system of eigenfunctions. As soon as we have the corresponding expansion at hand, we will show the equivalence between these eigenfunctions and the Cartesian multipole fields for cylindrical sources. Hence, this expansion will allow for a direct calculation of the desired multipole coefficients.

We will start by briefly deriving the mathematical background to decompose the scattered field of a single metaatom into multipole fields. As known from Mie's theory [17] the translational invariance in z-direction allows to separate the general vectorial scattering problem into the two scalar cases of TE- and TM-polarization. For light propagating in a linear, homogenous, isotropic, local medium the tangential fields satisfy the scalar wave equation [18]

$$\nabla^2_{x,y} F_z(x,y) + k(\omega)^2 F_z(x,y) = 0 \tag{1}$$

with $k(\omega)^2 = \omega^2/c^2$. In Eq. (1) $F_z(x,y)$ denotes the tangential component of either the magnetic field for TM polarization (magnetic component out-of-plane) or the electric field for TE polarization (electric field component out-of-plane).

Casting Eq. (1) into polar coordinates with $x = R\cos(\phi),\ y = R\sin(\phi),\ R = \sqrt{x^2+y^2}$ we

#126749 - $15.00 USD Received 9 Apr 2010; accepted 24 May 2010; published 22 Jun 2010

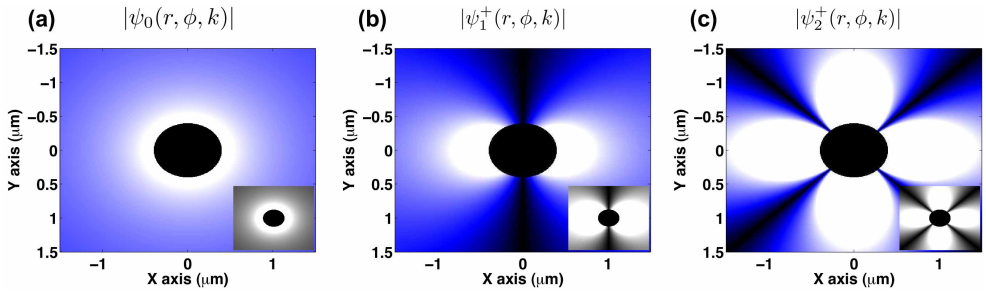

Fig. 1. (Color online) The modulus of the magnetic field distribution (TM polarization) described by the eigenfunctions according to Eq. (5) for the first three expansion orders. We have plotted the eigenfunctions accounting for the $\cos(m\phi)$ angular distributions only. The results for the $\sin(m\phi)$ terms would result in a rotation by an angle of $\pi/2m$. By comparison with the field distributions of point multipoles, which are shown in the gray-scaled insets, it can already be anticipated that the eigenfunctions ψ can be identified with multipole fields. Here $m = 0$ (a) corresponds to a magnetic dipole, $m = 1$ (b) is related to the electric dipole, while the electric quadrupole is associated with $m = 2$ (c).

obtain $[F_z = F_z(R,\phi)]$

$$\frac{1}{R}\frac{\partial}{\partial R}\left(R\frac{\partial}{\partial R}F_z\right)+\frac{1}{R^2}\left(R\frac{\partial^2}{\partial\phi^2}F_z\right)+k^2F_z=0. \tag{2}$$

The general solutions to this equation are radially dependent Bessel functions with an azimuthally varying phase

$$F_z=\sum_{m=-\infty}^{\infty}Z_m(kR)e^{im\phi}. \tag{3}$$

Equation (3) corresponds to the linearly independent solutions of Eq. (2) which consist of combinations of Bessel functions of the first $[J_m(kR)]$ and the second kind $[Y_m(kR)]$ denoted as Z_m multiplied by an angular function. Finally the scattered field from any cylindrical object centered at the origin and subject to the Sommerfeld radiation condition at infinity reads as

$$F_{z,s}=\sum_{m=-\infty}^{\infty}a_m i^m H_m^{(1)}(kR)e^{im\phi}, \tag{4}$$

where $H_m^{(1)}(kR)=J_m(kR)+iY_m(kR)$ are Hankel functions of the first kind and a_m are the expansion coefficients, termed Mie scattering coefficients of the respective expansion order m. Note that any field outside a virtual cylinder that entirely contains the scattering object can be expressed by Eq. (4) since these eigensolutions form an orthogonal and complete set of eigenfunctions. By expanding the field scattered by an arbitrary particle in this base we can determine the contribution of the respective expansion order m to the total scattered field.

The individual scattering order m always consists of two parts, namely the contributions from

#126749 - $15.00 USD
Received 9 Apr 2010; accepted 24 May 2010; published 22 Jun 2010

m and $-m$ in Eq. (4). Hence the scattered field ($F_{z,s}$) summarizing these orders can be rewritten

$$\begin{aligned} F_{z,s} &= \sum_{m=0}^{\infty} \left[a_m^+ \psi_m^+(R,\phi,k) + a_m^- \psi_m^-(R,\phi,k) \right], \\ \psi_m^+(R,\phi,k) &= i^m H_m^{(1)}(kR)\cos(m\phi), \\ \psi_m^-(R,\phi,k) &= i^{m+1} H_m^{(1)}(kR)\sin(m\phi), \\ a_m^\pm &= (a_m \pm a_{-m}), \end{aligned} \tag{5}$$

where we used $[H_m^{(1)} = H_{-m}^{(1)}]$. Now Eq. (5) can be considered as an usual series expansion with respect to eigenfunctions of increasing order. These eigenfunctions $\psi_m^\pm(R,\phi,k)$ are simply products of a radially and an azimuthally varying function. Regarding the azimuthal terms it can be seen from Eq. (5) that they split into two contributions that are $\pi/2m$ phase-shifted indicated by the superscripts $\pm$, respectively. This is related to the fact that each expansion order is composed of two physically identical but azimuthally rotated contributions of order m. For realistic metaatoms the fundamental azimuthal part can be selected regarding the symmetries of the nanostructure; in general both linear independent contributions have to be considered for the respective order m.

In order to decompose the scattered field of an arbitrary metaatom into the derived set of eigenfunctions [Eqs.(5)] the Mie coefficients a_m are required. As usual they are obtained by evaluating the overlap integral between the eigenfunction $\psi_m^\pm(R,\phi,k)$ and the respective field component $F_z(R,\phi)$ of the individual scattering object

$$a_m^\pm = \frac{\int_0^{2\pi} d\phi \int_{R_1}^{R_2} dR R F_z(R,\phi) \psi_m^{\pm\dagger}(R,\phi,k)}{\int_0^{2\pi} d\phi \int_{R_1}^{R_2} dR R |\psi_m^\pm(R,\phi,k)|^2}. \tag{6}$$

With Eq. (6) it is possible to rigorously determine $a_m^\pm$ based on the field overlap calculated on an annulus with the two radii R_2 and R_1. Here the orthogonality of the eigenfunctions $\psi_m^\pm(R,\phi,k)$ was exploited, i.e. replacing $F_z(R,\phi)$ by any eigenfunction of the order l such that $F_z(R,\phi) = \psi_l(R,\phi,k)$ yields

$$\begin{aligned} & \frac{\int_0^{2\pi} d\phi \int_{R_1}^{R_2} dR R \psi_l^\pm(R,\phi,k) \psi_m^{\pm\dagger}(R,\phi,k)}{\int_0^{2\pi} d\phi \int_{R_1}^{R_2} dR R |\psi_m(R,\phi,k)|^2} \\ = & \frac{\int_{R_1}^{R_2} dR R H_l^{(1)}(R,k) H_m^{(1)}(R,k)}{\int_0^{2\pi} d\phi \int_{R_1}^{R_2} dR R |\psi_m(R,\phi,k)|^2} \int_0^{2\pi} d\phi \left[\sin(l\phi)\sin(m\phi) + \cos(l\phi)\cos(m\phi) \right], \\ = & \frac{\int_{R_1}^{R_2} dR R H_l^{(1)}(R,k) H_m^{(1)}(R,k)}{\int_{R_1}^{R_2} dR R |H_m^{(1)}(kR)|^2} \delta_{ml} = \delta_{ml}. \end{aligned} \tag{7}$$

By exploiting the orthogonality of the azimuthally varying part of $\psi_m^\pm(R,\phi,k)$, it suffices to evaluate the overlap integral for a fixed value of R rather than an annulus to obtain $a_m^\pm$ [18]. However, it turned out that for numerically (or potentially experimentally) determined scattered fields of realistic metaatoms, the annulus integration is more stable and it was hence retained. This is not a numerical inaccuracy but it is rather attributed to the discrete mesh where the numerical data is available. This mesh is not aligned with a cylinder surrounding the object and an appropriate interpolation is required. Although a sufficiently fine grid improves the stability this issue can be circumvented if the annulus integration is performed.

#126749 - $15.00 USD Received 9 Apr 2010; accepted 24 May 2010; published 22 Jun 2010

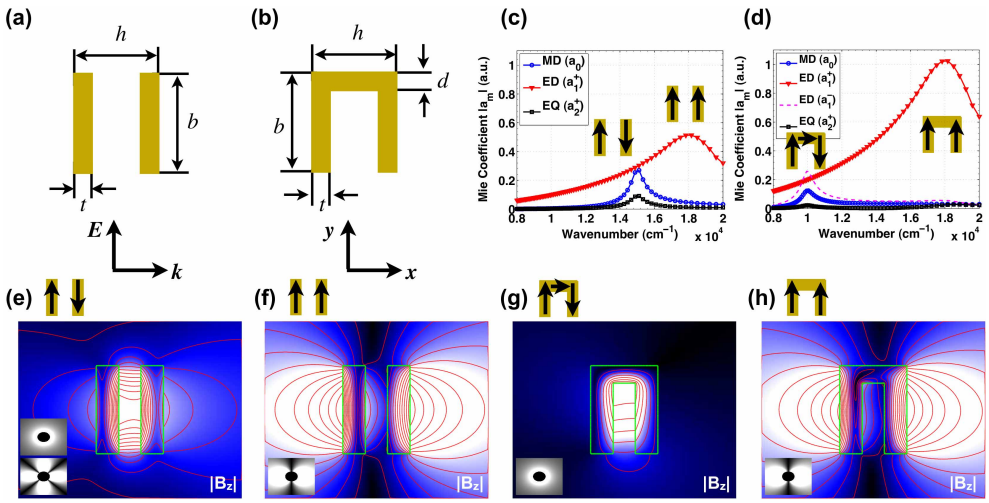

Fig. 2. (Color online) The illumination conditions, the orientation, and the definition of the geometrical parameters of the CW (a) and the SRR metaatom (b). The calculated Mie coefficients, related to the magnetic dipole (MD), the electric dipole (ED) and the electric quadrupole (EQ) for the CW (c) and the SRR (d) metaatom. Finally, the scattered magnetic fields for the *magnetic* (e) and the *electric* resonance (f) of the CW and the SRR (g,h) are shown, respectively. The gray-scaled insets show the exact multipole magnetic field distributions as in Fig. 1 to underline the similarities to the exact scattering field patterns.

Although, it suffices to know the amplitudes $a_m^{\pm}$ to fully describe the scattering response, they do not provide the physical insight as provided by Cartesian multipole moments. Therefore, they need to be unambiguously related. Since we have restricted ourselves to a two-dimensional configuration, we have to relate the scattered field of a line source exhibiting any of the relevant electric or magnetic multipole moments to the respective cylindrical eigenfunctions. Starting with the well-known expressions for electrodynamic point multipoles in Cartesian coordinates [18, 19] we derive below how they are related to $\psi_m(R,\phi,k)$. This is performed for the three lowest orders by integrating the point multipoles in Cartesian coordinates along the z-direction to disclose the radiation pattern of a line source exhibiting such point multipoles.

The vector potential of monochromatic electromagnetic fields originating from localized oscillating currents for the two lowest orders of a multipole expansion reads as

$$\mathbf{A}(\mathbf{r}) \quad = \quad \frac{\mu_0}{4\pi}\frac{e^{ikr}}{r}\int d^3r'\mathbf{j}(\mathbf{r}') + \frac{\mu_0}{4\pi}\frac{e^{ikr}}{r}\left(\frac{1}{r}-ik\right)\int d^3r'\mathbf{j}(\mathbf{r}')(\mathbf{n}\cdot\mathbf{r}'). \tag{8}$$

The first term in Eq. (8) accounts for the electric dipole moment where r is the length of the three dimensional radius vector $(r=\sqrt{x^2+y^2+z^2})$ and $\mathbf{n}=\mathbf{r}/r$ is the normal vector. The second term consists of the electric quadrupole and the magnetic dipole contributions, both representing second-order moments in the multipole expansion. After some algebra the electric dipole term can be written as [18]

$$\mathbf{A}_{\mathrm{ed}}(\mathbf{r}) \quad = \quad -i\omega\frac{\mu_0}{4\pi}\frac{e^{ikr}}{r}\mathbf{p}(\mathbf{r}), \tag{9}$$

with $\mathbf{p}(\mathbf{r})=\int d^3r'\mathbf{r}'\rho(\mathbf{r}')$ being the electric dipole moment. For electric dipole moments local-

#126749 - $15.00 USD
Received 9 Apr 2010; accepted 24 May 2010; published 22 Jun 2010

ized in the (x,y) plane the z component of the magnetic field can be calculated as

$$\begin{aligned} \mathbf{B}(\mathbf{r}) &= \nabla \times \mathbf{A}(\mathbf{r}), \\ B_{\mathrm{ed,z}}(\mathbf{r}) &= -i\omega \frac{\mu_0}{4\pi} \frac{e^{ikr}}{r} \left[p_y \left(iky - \frac{y}{r^2} \right) - p_x \left(ikx - \frac{x}{r^2} \right) \right]. \end{aligned} \tag{10}$$

Since we are interested in the two-dimensional representation of the fields we integrate Eq. (10) along the z axis (see appendix for details)

$$\begin{aligned} B^{\mathrm{2D}}_{\mathrm{ed,z}}(x,y) &= \omega \frac{\mu_0 k}{4} \left[\cos(\phi) p_x - \sin(\phi) p_y \right] H_1^{(1)}(kR), \\ &= H_1^{(1)}(kR) \left[a_1^+ \cos(\phi) - a_1^- \sin(\phi) \right], \\ a_1^{\pm} &\equiv \frac{\omega \mu_0}{4} p_{x,y}. \end{aligned} \tag{11}$$

As can be easily verified, this electric dipole field coincides with the field in Eq. (5) for $m = 1$. Hence, the eigenfunction of the order $m = 1$ represents the electric dipole contribution. Likewise one can show that the magnetic dipole and the electric quadrupole contribution correspond to $m = 0$ and $m = 2$, respectively. A detailed derivation for the multipoles can be found in the appendix. Based on these results we can conclude that simply by calculating the Mie coefficients $a_m^{\pm}$ we have the multipole coefficients of the scattered field at hand.

In Fig. 1 the magnetic field patterns for $m = 0, 1, 2$ are shown. Obviously they correspond to the known field distributions for the magnetic dipole ($m = 0$), the electric dipole ($m = 1$) and the electric quadrupole ($m = 2$) as is clear by comparison with the field patterns of point multipoles (see insets in Fig. 1).

Having finished the analytical treatment, we are going to apply the results to exemplarily reveal the multipole scattering contributions for two prominent metaatoms in the following.

3. Multipole scattering of Metaatoms

For the application of the technique developed above, we selected the CW and the SRR geometry. We emphasize that this is not a necessary restriction because arbitrary structures can be investigated too with the developed formalism. We selected these two structures since several modified, more complex metamaterials are composed out of these basic plasmonic entities [4, 5, 12, 20]. The investigated metaatoms for both scenarios are shown in Fig. 2(a,b). The CW structure has a wire distance of $h = 60$ nm, a wire thickness of $t = 20$ nm and a width of $b = 100$ nm. To evaluate the overlap integral the annulus radii were set to $R_1 = 70$ nm and $R_2 = 80$ nm. In order to observe the localized eigenmodes at similar spectral positions we used the same dimensions for the SRR with an additional connection ($d = 20$ nm) of both wires [Fig. 2(b)]. As a material for both metaatoms we selected gold [21] embedded in vacuum. The structures were illuminated according to the conditions as shown in Fig. 2(a,b) with monochromatic plane waves.

In order to calculate the electromagnetic near fields we applied the finite element method [22]. By calculating the scattering patterns for both structures and performing the field overlap calculations according to Eq. (8) for the first three orders one obtains the Mie coefficients as shown in Fig. 2(c,d). For both metaatoms the observed low energy resonance peaks occur for both second order multipole contributions (electric quadrupole and magnetic dipole) at the same frequency (wavenumber), while the high frequency resonances are associated with the electric dipole modes. Thus, the usual argument that the electric dipole contribution of the two currents, oscillating π out-of-phase in the wires perpendicular to the propagation direction, annihilate and hence the next higher order multipole moments prevail, is confirmed by these

#126749 - $15.00 USD Received 9 Apr 2010; accepted 24 May 2010; published 22 Jun 2010

results. Furthermore, the quantitative contribution of each multipole moment is clearly revealed. For the CW structure [Fig. 2(c)] the electric quadrupole contribution is much stronger than that for the SRR. This is due to the different symmetry of both metaatoms. The shortcut of both wires essentially prevents the excitation of a quadrupole moment. Hence, the SRR's optical response is mainly governed by the electric and the magnetic dipole moment.

This argumentation is supported by considering the near fields at resonance. Comparing the pure multipole fields (Fig. 1) with the scattered fields of the two metaatoms [Fig. 2(e-h)] it becomes obvious that the magnetic field of the high frequency resonance (electric resonance) is very similar to that of an electric dipole. The scattered magnetic fields for the low frequency resonance (magnetic resonance) for the CW structure shows a combination of centro-symmetric magnetic dipole fields between the wires and the electric quadrupole fields around. This is indicated by the fourfold patterns in the iso-surface lines in Fig. 2(e) outside the CW geometry. Differing from these patterns the SRR exhibits near field features that manly attributed to the magnetic dipole radiation pattern [Fig. 2(g)]. In addition a weak background contribution of an electric dipole tilted by 45° can be observed in Fig. 2(g), caused by the superposition of weak SRR electric dipole moments in x and y directions [e.g. see Fig. 2(d)].

Note that with the knowledge of the scattering response of the isolated metaatoms other physical observables become easily accessible. Most notably various other important metamaterial properties, i.e. the effective cross sections [23] or the isolated polarizabilities [24] that can be obtained by this Mie theory based formalism straightforwardly, can be analytically calculated [25].

Finally, the dependence of the multipole coefficients on the choice of the origin is investigated. From electrostatics it is known that the first non-vanishing multipole moment does not depend on the choice of the origin. For optical fields this is not valid anymore. However, for the scattering response of very small nanoparticles where the quasi-static approximation is valid, this dependency is expected to be negligible for reasonably chosen origins. Exemplarily the multipole expansion is performed for the scattered field of a SRR with smaller dimensions ($h = 70\ nm,\ b = 70\ nm,\ t = 25\ nm,\ d = 20\ nm$) to prove the quasi-statically expected behavior for three different origins. The corresponding results are shown in Fig. 3. Clearly the electric dipole moments are almost constant for different origins, whereas the magnetic dipole as well as the electric quadrupole moments may appreciably deviate, in particular for the second resonance. Of course, the multipole moments will strongly deviate from the results shown here if the origin is placed far outside the metaatoms, but then any multipole expansion becomes meaningless, too. Physically, the origin should be chosen such that all higher order multipoles beyond the second order are strongly suppressed.

Nevertheless from these results we can conclude that for reasonably chosen origins, i.e. placed close to the center of mass as suggested [14] the multipolar character of the scattered field can be revealed consistently. For calculating effective material parameters on the other hand this origin dependence has to be kept in mind [19].

4. Summary

In summary, we presented a novel technique based on Mie theory to retrieve the contributions of various multipole excitations to the near-field scattering pattern of metaatoms. For the sake simplicity we restricted ourselves to two-dimensional metaatoms. Since Mie theory has been originally developed for three-dimensional objects (spheres) the approach can be also extended towards three-dimensional metaatoms. With the presented formalism we revealed the quantitative contributions of multipole moments to the plasmonic eigenmodes of the cut-wire and the split-ring resonator structures. As previously phenomenologically interpreted, due to the similarities of the multipole moments and the electron dynamics, we could rigorously confirm the

#126749 - $15.00 USD Received 9 Apr 2010; accepted 24 May 2010; published 22 Jun 2010

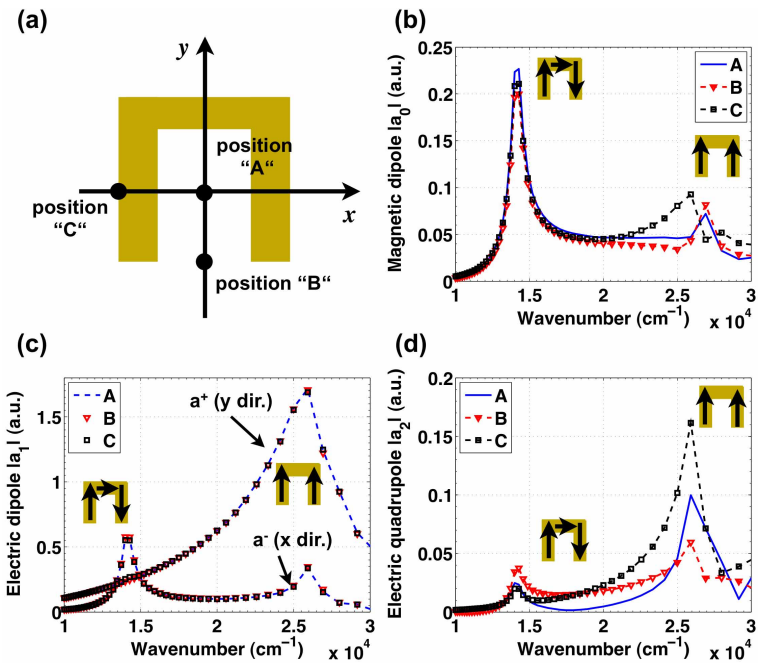

Fig. 3. (Color online) (a) The SRR geometry together with the three positions representing the selected origins for the multipole expansion. "A" is associated with the center of symmetry of the corresponding CW structure, while "B" and "C" represent additional positions out of the metaatoms center. The calculated Mie coefficients for the magnetic dipole (MD)(b),the electric dipole (ED) (c) and the electric quadrupole (EQ) (d). For completeness both electric dipole moments along the x (a_1^+) and the y axis (a_1^-) are shown.

excitation of up to second order multipoles as the dominant scattering contributions. We anticipate that such a multipole expansion of the scattered field is a genuine approach to optimize isolated metaatoms with regard to a predefined scattering response, e.g. optical magnetism in terms of magnetic dipole contributions. It will be very helpful to identify the effect of periodicity or its absence, in case of metamaterials fabricated with self-organization techniques, with respect to the effective MM properties. Beyond possible applications in the field of metamaterials, the presented approach may also provide guidelines in the design of optical nanoantennas to achieve a desired radiation characteristics to be matched to an, in principle, arbitrary source.

A. Appendix: The connection between 3D and 2D radiated multipole fields

A.1. Electric dipole

We start our considerations with the vector potential for the first two expansion orders Eq. (8)

$$\mathbf{A}(\mathbf{r}) \quad = \quad \frac{\mu_0}{4\pi}\frac{e^{ikr}}{r}\int d^3r'\mathbf{j}(\mathbf{r}') + \frac{\mu_0}{4\pi}\frac{e^{ikr}}{r}\left(\frac{1}{r}-ik\right)\int d^3r'\mathbf{j}(\mathbf{r}')(\mathbf{n}\cdot\mathbf{r}'). \tag{12}$$

At first we consider the first order term on the right hand side of Eq. (12) which represents the electric dipole contribution. Applying the continuity equation and requiring that the current

#126749 - $15.00 USD
Received 9 Apr 2010; accepted 24 May 2010; published 22 Jun 2010

density vanishes at infinity, we arrive at the well-known vector potential of an electric dipole

$$\mathbf{A}_{\mathrm{ed}}(\mathbf{r}) = -i\omega\frac{\mu_0}{4\pi}\frac{e^{ikr}}{r}\mathbf{p}(\mathbf{r}). \tag{13}$$

According to Maxwell's equations we obtain the z-component of the magnetic field by applying the curl operator to the potential [Eq. (13)]

$$\begin{aligned} B_{\mathrm{ed},z}(\mathbf{r}) &= \frac{\partial}{\partial x}A_y(\mathbf{r}) - \frac{\partial}{\partial y}A_x(\mathbf{r}), \\ &= -i\omega\frac{\mu_0}{4\pi}\left(p_y\frac{\partial}{\partial x} - p_x\frac{\partial}{\partial y}\right)\frac{e^{ikr}}{r}. \end{aligned} \tag{14}$$

In order to obtain the associated two-dimensional fields we integrate the three-dimensional fields along the z axis. This is equivalent to the transition from *point* multipoles to *line* multipoles, similar to the transition from the three-dimensional to the two-dimensions Green's function. [26]

$$\begin{aligned} B^{\mathrm{2D}}_{\mathrm{ed},z}(x,y) &= \int_{-\infty}^{\infty} dz B_{\mathrm{ed},z}, \\ &= -i\omega\frac{\mu_0}{4\pi}\left(p_y\frac{\partial}{\partial x} - p_x\frac{\partial}{\partial y}\right)\int_{-\infty}^{\infty} dz\frac{e^{ikr}}{r}. \end{aligned} \tag{15}$$

The integral can be carried out with the help of Eq. 8.421 in [27]

$$\int_{-\infty}^{\infty} dz\frac{e^{ik\sqrt{R^2+z^2}}}{\sqrt{R^2+z^2}} = i\pi H_0^{(1)}(kR). \tag{16}$$

Now the recursion formula for Hankel's functions of the first kind can be applied to calculate the remaining derivatives

$$\begin{aligned} \frac{\partial}{\partial z}H_n^{(1)}(z) &= \frac{n}{z}H_n^{(1)}(z) - H_{n+1}^{(1)}(z), \\ \frac{\partial}{\partial X_l}H_0^{(1)}(kR) &= -H_1^{(1)}(kR)\frac{X_l k}{R},\ X_l \in \{x,y\}, \end{aligned} \tag{17}$$

which allows to calculate the required magnetic fields as

$$B^{\mathrm{2D}}_{\mathrm{ed},z}(R,\phi) = \omega\frac{\mu_0 k}{4}\left[\cos(\phi)p_x - \sin(\phi)p_y\right]H_1^{(1)}(kR). \tag{18}$$

According to Eq. (5) the associated magnetic field for $m = 1$ is given by

$$\begin{aligned} F_{z,s} &= a_1^+\psi_1^+(R,\phi,k) + a_1^-\psi_1^-(R,\phi,k), \\ &= \left[a_1^+\cos(\phi) - a_1^-\sin(\phi)\right]H_1^{(1)}(kR). \end{aligned} \tag{19}$$

It becomes obvious that the coefficients $a_1^{\pm}$ represent two electric dipoles rotated by $\pi/2$, since a comparison of the coefficient between Eq. (18) and Eq. (19) yields

$$a_1^+ = \omega\frac{\mu_0 k}{4}p_x, \qquad a_1^- = \omega\frac{\mu_0 k}{4}p_y. \tag{20}$$

#126749 - $15.00 USD Received 9 Apr 2010; accepted 24 May 2010; published 22 Jun 2010

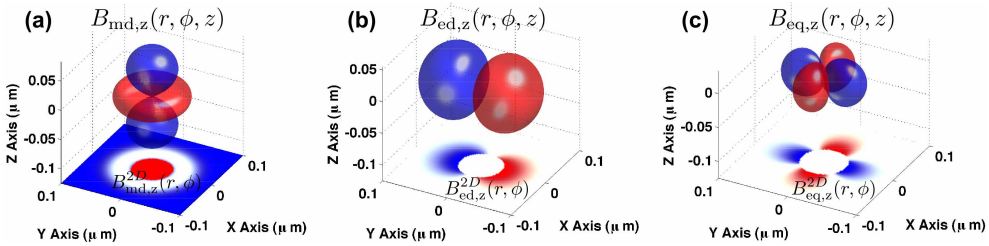

Fig. 4. (Color online) The exact field patterns for the z component of the magnetic field for the magnetic dipole (a), the electric dipole (b), and the electric quadrupole (c) for carrier dynamics in the (x,y) plane. The two-dimensional field distributions below the three-dimensional ones show the three-dimensional fields for the respective multipole moment integrated along the z axis. The moduli of these two-dimensional fields correspond to the insets in Fig. 1(a-c) and precisely agree with $\psi_m(r,\phi)$, $m \in \{1,2,3\}$, respectively as shown in the derivation below.

A.2. Magnetic dipole

The second order expansion term in Eq. (12) can be split into two contributions where one is associated with the vector potential of the electric quadrupole and the other one with the magnetic dipole. Hence, both quantities represent second-order moments

$$\begin{aligned}
\mathbf{A}(\mathbf{r}) &= \frac{\mu_0}{4\pi}\frac{e^{ikr}}{r}\left(\frac{1}{r}-ik\right)\int d^3r'\mathbf{j}(\mathbf{r}')(\mathbf{n}\cdot\mathbf{r}') \\
&= \mathbf{A}_{\mathrm{md}}(\mathbf{r})+\mathbf{A}_{\mathrm{eq}}(\mathbf{r}), \\
\mathbf{A}_{\mathrm{eq}}(\mathbf{r}) &= \frac{\mu_0}{4\pi}\frac{e^{ikr}}{r}\left(\frac{1}{r}-ik\right)\underbrace{\int_{-\infty}^{\infty} d^3r'\frac{1}{2}\left[(\mathbf{n}\cdot\mathbf{r}')\mathbf{j}(\mathbf{r}')+(\mathbf{n}\cdot\mathbf{j}(\mathbf{r}'))\mathbf{r}'\right]}_{\propto\mathbf{Q}}, \\
\mathbf{A}_{\mathrm{md}}(\mathbf{r}) &= \frac{\mu_0}{4\pi}\frac{e^{ikr}}{r}\left(\frac{1}{r}-ik\right)\underbrace{\left[\frac{1}{2}\int_{-\infty}^{\infty} d^3r'\mathbf{r}'\times\mathbf{j}(\mathbf{r}')\right]}_{\equiv\mathbf{m}}\times\mathbf{n} \\
&= \frac{\mu_0}{4\pi}\frac{e^{ikr}}{r}\left(\frac{1}{r}-ik\right)\mathbf{m}\times\mathbf{n}. \qquad (21)
\end{aligned}$$

Currents in the (x,y) plane only induce a magnetic dipole moment $\mathbf{m}$ pointing into z direction

$$\mathbf{A}_{\mathrm{md}}(\mathbf{r}) = \frac{\mu_0}{4\pi}\frac{e^{ikr}}{r^2}\left(\frac{1}{r}-ik\right)(-y\mathbf{e}_x+x\mathbf{e}_y)\,m_z. \qquad (22)$$

Using the identity

$$\frac{\partial}{\partial X_j}\frac{e^{ikr}}{r} = -X_j\frac{e^{ikr}}{r^2}\left(\frac{1}{r}-ik\right),\ X_j\in\{x,y\}, \qquad (23)$$

Eq. (22) can be simplified yielding

$$\mathbf{A}_{\mathrm{md}}(\mathbf{r}) = \frac{\mu_0 m_z}{4\pi}\left(\mathbf{e}_x\frac{\partial}{\partial y}-\mathbf{e}_y\frac{\partial}{\partial x}\right)\frac{e^{ikr}}{r}. \qquad (24)$$

#126749 - $15.00 USD
Received 9 Apr 2010; accepted 24 May 2010; published 22 Jun 2010

In order to get the magnetic field Eq. (14) can be applied which has to be integrated along the z axis as for the electric dipole before

$$B_{\mathrm{md},z}(\mathbf{r}) = -\frac{\mu_0 m_z}{4\pi}\left(\frac{\partial^2}{\partial x^2}+\frac{\partial^2}{\partial y^2}\right)\frac{e^{ikr}}{r}. \quad (25)$$

Equation (25) can be easily integrated applying again Eq. (16)

$$B^{\mathrm{2D}}_{\mathrm{md},z}(x,y) = i\frac{\mu_0\mu(\omega)m_z}{4}k^2\left[\frac{2}{kR}H_1^{(1)}(kR)-H_2^{(1)}(kR)\right], \quad (26)$$

which can be simplified using the theorem 8.473, 3 in [27]

$$H_0^{(1,2)}(z) = \frac{2}{z}H_1^{(1,2)}(z)-H_2^{(1,2)}(z), \quad (27)$$

resulting in the expected radially dependent expression for the scattered magnetic field

$$B^{\mathrm{2D}}_{\mathrm{md},z}(R,\phi) = i\frac{\mu_0 m_z k^2}{4}H_0^{(1)}(kR). \quad (28)$$

For comparison Eq. (5) with $m=0$ yields

$$F_{x,s} = a_0 H_0^{(1)}(kR). \quad (29)$$

Comparing Eq. (28) and Eq. (29) we see that the coefficient a_0 again is directly proportional to the magnetic dipole moment, similar to the electric dipole moment before [Eq. (20)]. Here the second term connected to a rotated magnetic dipole by $\pi/2$ vanishes, as expected for the radial symmetric radiation pattern of a magnetic dipole.

Electric quadrupole

The second term connected to the electric quadrupole moment in the vector potential of Eq. (21) can be simplified using Gauss' law and the continuity equation to [18]

$$\mathbf{A}_{\mathrm{eq}}(\mathbf{r}) = -i\omega\frac{\mu_0}{8\pi}\frac{e^{ikr}}{r}\left(\frac{1}{r}-ik\right)\int_{-\infty}^{\infty}d^3r'\mathbf{r}'(\mathbf{n}\cdot\mathbf{r}')\rho(\mathbf{r}'). \quad (30)$$

In the following we restrict the carrier dynamics to the (x,y) plane that might be expressed by

$$\rho(\mathbf{r}') = \sum_{\alpha=1}^{N} q_\alpha \delta[x'-x_\alpha(t)]\delta[y'-y_\alpha(t)]\delta(z'). \quad (31)$$

We now rewrite the integral kernel of Eq. (30)

$$\int_{-\infty}^{\infty}d^3r'\mathbf{r}'(\mathbf{n}\cdot\mathbf{r}')\rho(\mathbf{r}') = \sum_{j=1}^{3}\mathbf{e}_j\sum_{l=1}^{3}\int_{-\infty}^{\infty}d^3r'X'_j n_l X'_l\rho(\mathbf{r}') \equiv \hat{Q}_{jl}(\mathbf{n})\mathbf{e}_j. \quad (32)$$

Here we have used $\hat{Q}(\mathbf{n})$

$$\hat{Q}(\mathbf{n}) = \sum_{\alpha=1}^{N} q_\alpha \begin{pmatrix} x_\alpha^2 n_x & x_\alpha y_\alpha n_y & 0 \\ y_\alpha x_\alpha n_x & y_\alpha^2 n_y & 0 \\ 0 & 0 & 0 \end{pmatrix} \equiv \begin{pmatrix} Q_{xx}n_x & Q_{xy}n_y & 0 \\ Q_{xy}n_x & Q_{yy}n_y & 0 \\ 0 & 0 & 0 \end{pmatrix}, \quad (33)$$

#126749 - $15.00 USD Received 9 Apr 2010; accepted 24 May 2010; published 22 Jun 2010

where the Q_{ij} are the primitive symmetric quadrupole tensor entries [19]. Substituting Eq. (33), (32) into Eq. (30) and applying Eq. (23) we obtain the vector potential

$$\mathbf{A}_{\mathrm{eq}}(\mathbf{r}) = i\omega\frac{\mu_0}{8\pi}\left[\mathbf{e}_x\left(Q_{xx}\frac{\partial}{\partial x}+Q_{xy}\frac{\partial}{\partial y}\right)+\mathbf{e}_y\left(Q_{yx}\frac{\partial}{\partial x}+Q_{yy}\frac{\partial}{\partial y}\right)\right]\frac{e^{ikr}}{r}. \quad (34)$$

This equation can again be used to calculate the respective magnetic field [Eq. (14)]

$$B_{\mathrm{eq},z}(\mathbf{r}) = i\omega\frac{\mu_0}{8\pi}\left[Q_{yx}\left(\frac{\partial^2}{\partial x^2}-\frac{\partial^2}{\partial y^2}\right)+Q_{yy}\frac{\partial^2}{\partial x\partial y}-Q_{xx}\frac{\partial}{\partial y\partial x}\right]\frac{e^{ikr}}{r}. \quad (35)$$

In a final step Eq. (25) can be integrated by applying Eq. (16)

$$B^{\mathrm{2D}}_{\mathrm{eq},z}(x,y) = -\omega\frac{\mu_0}{8}\left[Q_{xy}\left(\frac{\partial^2}{\partial x^2}-\frac{\partial^2}{\partial y^2}\right)+(Q_{yy}-Q_{xx})\frac{\partial^2}{\partial x\partial y}\right]H_0^{(1)}(kR), \quad (36)$$

which can be simplified using the recursion formula Eq. (17) for the second derivatives

$$B^{\mathrm{2D}}_{\mathrm{eq},z}(R,\phi) = -\omega\frac{\mu_0 k^2}{8}\left\{Q_{xy}[\cos^2(\phi)-\sin^2(\phi)]+(Q_{yy}-Q_{xx})\cos(\phi)\sin(\phi)\right\}H_2^{(1)}(kR). \quad (37)$$

Finally we end up with the magnetic field

$$B^{\mathrm{2D}}_{\mathrm{eq},z}(R,\phi) = -\omega\frac{\mu_0 k^2}{16}[Q_{xy}\cos(2\phi)+(Q_{yy}-Q_{xx})\sin(2\phi)]H_2^{(1)}(kR). \quad (38)$$

The evaluation of Eq. (5) for $m=2$ yields

$$F_{z,s} = -\left[a_2^{+}\cos(2\phi)+ia_2^{-}\sin(2\phi)\right]H_2^{(1)}(kR). \quad (39)$$

Again the coefficients $a_2^{\pm}$ are proportional to the electric quadrupole moment expressions under consideration.

Acknowledgements

Financial support by the Federal Ministry of Education and Research (MetaMat and PhoNa), the State of Thuringia within the Pro-Excellence program (MeMa), and the European Union (NANOGOLD) is acknowledged. Part of the work of JY was supported by the Erasmus Mundus Master Program OpSciTech. The work was furthermore supported by the DAAD and the French MESR within the PROCOPE exchange program.

#126749 - $15.00 USD Received 9 Apr 2010; accepted 24 May 2010; published 22 Jun 2010